
MARINE MICROALGAE DETECTION IN MICROSCOPY IMAGES: A NEW DATASET

Shizheng Zhou
Hainan University
Haikou, China 570100
xpzzsz@hotmail.com

Juntao Jiang
Zhejiang University
Hangzhou, China 310058
juntaojiang@zju.edu.cn

Xiaohan Hong
The State University of New York at Stony Brook
Stony Brook, USA 11790
xiaohan.hong@stonybrook.edu

Yajun Fang
Universal Village Society
Boston, USA 02101
yjfang@universal-village.org

Yan Hong
Hainan University
Haikou, China 570100
yanhong@hainanu.edu.cn

Pengcheng Fu
Hainan University
Haikou, China 570100
pcfu@hainanu.edu.cn

November 15, 2022

ABSTRACT

Marine microalgae are widespread in the ocean and play a crucial role in the ecosystem. Automatic identification and location of marine microalgae in microscopy images would help establish marine ecological environment monitoring and water quality evaluation system. A new dataset for marine microalgae detection is proposed in this paper. Six classes of microalgae commonly found in the ocean (*Bacillariophyta*, *Chlorella pyrenoidosa*, *Platymonas*, *Dunaliella salina*, *Chrysophyta*, *Symbiodiniaceae*) are microscopically imaged in real-time. Images of *Symbiodiniaceae* in three physiological states known as normal, bleaching, and translating are also included. We annotated these images with bounding boxes using Labelme software and split them into the training and testing sets. The total number of images in the dataset is 937 and all the objects in these images were annotated. The total number of annotated objects is 4201. The training set contains 537 images and the testing set contains 430 images. Baselines of different object detection algorithms are trained, validated and tested on this dataset. This data set can be got accessed via tianchi.aliyun.com/competition/entrance/532036/information.

Keywords marine microalgae · object detection · data annotation · microscopic imaging · computer vision

1 Introduction

Marine microalgae are widely distributed in the ocean [1] as a part of the “blue carbon sink” that uses solar energy and dissolve CO₂ to produce oxygen as well as carbohydrates through photosynthesis [2]. They are thus involved in the global ocean-atmosphere carbon cycle to mitigate anthropogenic CO₂ emission, which is the leading cause of escalating climate change. Healthy and viable algal growth is critical to the prosperity of diverse marine ecosystems in the ocean and the carbon capture, utilization, and storage.

Also, species and quantities of microalgae are widely used as indicators for marine ecological environment monitoring, and water quality evaluation worldwide [3, 4, 5, 6, 7]. For example, *Symbiodiniaceae* are closely related to their host corals and thus affect the aquatic environment. For example, the species and density of *Symbiodiniaceae* can be analyzed to predict coral bleaching[8], which results from excessive production of reactive oxygen species (ROS) in the symbiotic algae family under excessive temperature or light [9, 10]. The diversity of *Symbiodiniaceae* also has potential relationship with coral thermal adaptability [11].

In order to monitor and determine the health status of marine microalgae *in situ*, integration of hardware and software is needed to enable real-time algal image acquisition, data analysis and implementation of machine learning algorithms to

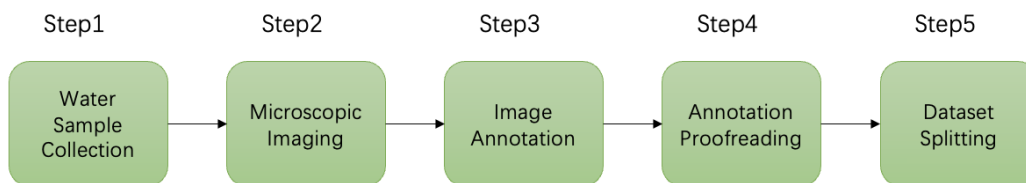


Figure 1: The workflow of producing the dataset for marine microalgae detection.

recognize and classify the cells of marine microalgae. Compared to current manual microscopic identification, which has problems of high professional level requirements, discontinuity of classifiers and time-consuming, automatic marine microalgae identification by using machine learning methods [12, 13, 14, 15, 16, 17, 18, 19] can meet the needs of rapid monitoring and provide convenience for researchers in marine and environmental science.

In this analysis of microalgae images, automatic localization and identification are expected to be achieved simultaneously, which would facilitate the downstream cells analysis. As the joint tasks of classification and localization, object detection can provide the basis for algae identification based on image information combined with biomorphological features. There have been some existing works [18, 19] applied algorithms in computer vision for microalgae detection and corresponding datasets.

In this study, we have taken samples of six classes of microalgae commonly found in the ocean (*Bacillariophyta*, *Chlorella pyrenoidosa*, *Platymonas*, *Dunaliella salina*, *Chrysophyta*, *Symbiodiniaceae*) and created an image dataset for them. We also collected the images of *Symbiodiniaceae* in different physiological states known as normal, bleaching and translating, and an image set of mixing all microalgae species described above. Since we will subsequently apply this dataset to the competition, the number of images containing *Bacillariophyta* was intentionally set lower than the others to examine how well the participants handled the problem of class imbalance in the dataset. In addition, we added an image set of mixed samples to the testing set, which was designed better to fit the algal samples in the field environment.

We hope to discover minimal differences between cells from a computer vision perspective and understand life’s heterogeneity, randomness and synergy at the single-cell level. We gave a brief description of the dataset information as well as the annotation process. Additionally, we trained some classical or state-of-the-art object detection methods as baselines on the training set and got a test result on the testing set.

Researchers are welcome to develop their own marine microalgae object detection algorithms on this dataset and compare their results with these baselines. We sincerely hope that this dataset of microscopy images for marine microalgae detection will not only boost related research on marine biology but also help establish future real-time monitoring and water quality evaluation system of the marine environment.

2 Related Works

2.1 Object Detection

Object Detection is a task of precisely estimating the concepts and locations of objects in each image [20, 21]. Traditional object detectors [22, 23, 24, 25] based on sophisticated handcrafted features used to be main-stream methods before the popularity of deep learning. Thanks to the capability of learning robust and high-level feature representations of images, Convolutional Neural Networks (CNNs) have been widely used in object detection. Two-stage detectors [26, 27, 28, 29, 30, 31, 32] achieved target region selection and detection in two steps while one-stage detector [33, 34, 35, 36, 37, 38, 39, 40, 41, 42] gave the class probabilities and position coordinate values of objects directly. Recently, some Transformer-based methods [43] were proposed, showing their strong ability in object detection. Commonly-used object datasets include Microsoft COCO [44] and Pascal VOC [45].

Some existing related works on microalgae microscopy images applied such a deep learning-based method. Cao et al. [19] used MobileNet [46] and SPP [27] to improve YOLOv3 while Park et al. [18] trained the YOLOv3 model with Darknet53 backbone [38].

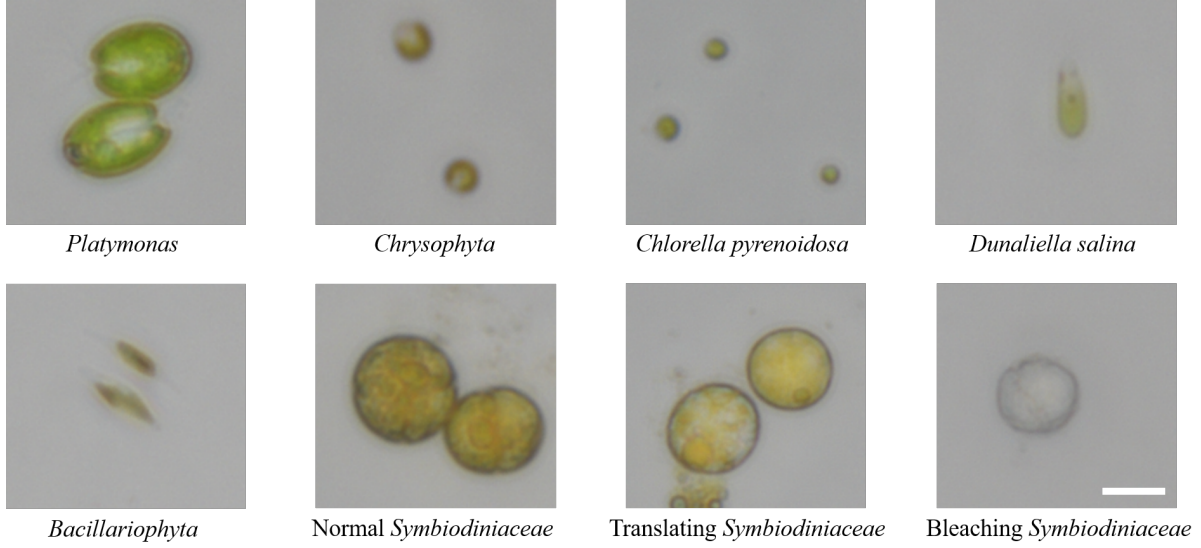


Figure 2: The images of six species of algae under 40× microscope lens of, including three physiological states of *Symbiodiniaceae*. Scale bar is 10 μm .

2.2 Microalgae Detection Dataset

Cao et al. [19] acquired microalgae images using a Nikon Ts2-FL/TS2 fluorescence microscope and then used the data augmentation methods to obtain a large number of images. The microalgae species in this dataset include *Prorocentrum lima* and *Karenia mikimotoi*. However, they failed to provide many details of this dataset, like producing process, the original resolution, and the total number of images and objects. Park et al. [38] collected 1,114 algae images with 3,663 objects collected by microscope (Eclipse Ni, NIKON, Japan). These images were split into 10, 20, or 30 genera to compare the model’s performance with different numbers of target objects for classification. Compared to existing works, our work not only builds a dataset with different species but attaches importance to *Symbiodiniaceae* in different physiological states, which is helpful to coral bleaching prediction and environment protection.

3 Dataset Production

This section will specifically describe the workflow of building this dataset. As Figure 1 shows, the workflow of the dataset production includes data(water samples containing different species of microalgae) collection, microscopic imaging, image annotation, annotation proofreading and splitting of the dataset into the training set and the testing set.

3.1 Data Collection

Microalgae samples collected in this study are common species in seawater, including *Platymonas*, *Chrysophyta*, *Chlorella pyrenoidosa*, *Dunaliella salina*, *Bacillariophyta* and *Symbiodiniaceae*, as shown in Figure 2. The algal samples were taken from collected fresh seawater and then were cultured in the medium.

- *Platymonas* is a genus of green algae in the family Volvocaceae [47] whose cell length is about 12 μm , and the algal body is flat and compressed. The cells are broadly ovate in front view, with a broad front end and a concave front of the top.
- *Chrysophyta*, also known as golden algae, is a kind of algae whose active cells are 4.4-7.1 μm long and 2.7-4.4 μm wide, with a dark red, oval eye spot located in the center of the cell, occasionally near the front of the cell.
- *Chlorella pyrenoidosa* is a kind of spherical unicellular algae in the Division Chlorophyta with a diameter of 3-8 μm , and without flagella.
- *Dunaliella salina* is a type of halophile green unicellular microalgae that is mainly found in hypersaline environments whose algal body is oval or pear-shaped, 18-28 μm long, 9.5-14 μm wide. Without a cell wall, the front of the cell is generally concave, and there is a cup-shaped chromophore in the algae.

- *Bacillariophyta* is a unicellular planktonic diatom with a siliceous cell wall. The cells are spindle-shaped, with an enlarged central part and acuminate at both ends, 12-23 μm long and 2-3 μm wide. Two yellow-brown pigment bodies flank the nucleus in the center of the cell.

The algae species mentioned above were collected from the Bohai Sea (Shangdong, China), isolated and purified by Fengyun Algae Co., Ltd., and cultured in an f/2 medium. The photo of the medium is shown in Figure 3.

- *Symbiodiniaceae*, also known as *Zooxanthella*, is a kind of algae establishing intracellular symbioses with organisms such as corals, anemones, jellyfish, nudibranchs, Ciliophora, Foraminifera, zoanthids and sponges [48]. It enters host cells by phagocytosis, persists as intracellular symbionts, multiplies and disperses into the environment.



Figure 3: The photo of seawater medium for microalgae cultivation

Symbiodiniaceae used to produce this dataset was kindly donated by a scholar and isolated from the Scleractinia coral *Galaxea fascicularis* in West Island (18°14'16", 109°21'54", Sanya, Hainan, China). There were two culture mediums for *Symbiodiniaceae*. The first culture medium was standard f/2 artificial seawater medium and the other in another 1L shaker's flask was stressed by heat shock at 40°C for about 2 hours to make the cells bleached.

Observed with a microscope, it was seen that the cells of normal *Symbiodiniaceae* were yellowish-brown, while the cells of bleaching *Symbiodiniaceae* were white, and the color of the translating cell was in between. There are minor differences in shape, size and structure between the three groups of *Symbiodiniaceae* cells.

Table 1: Information of various microalgae species in the dataset

Species	Size
<i>Platymonas</i>	12 μm cell length
<i>Chrysophyta</i>	4.4-7.1 μm long, 2.7-4.4 μm wide
<i>Chlorella pyrenoidosa</i>	3-8 μm diameter
<i>Dunaliella salina</i>	18-28 μm long, 9.5-14 μm wide
<i>Bacillariophyta</i>	12-23 μm long and 2-3 μm wide
<i>Symbiodiniaceae</i>	10-15 μm diameter

3.2 Image Acquisition and Annotation

Image acquisition and processing are based on an inverted microscopic imaging platform. In our work, a high-definition camera (DS-FI3, Nikon, Japan) with a viewing field of 7.18×5.32 mm and a 5.9-megapixel complementary metal-oxide-semiconductor (CMOS) image sensor are attached to the inverted microscope. It can capture images with a resolution of up to 2880×2048 pixels and transfer them via a USB 3.0 port. The exposure time is set to 1 μs . The photo of the device is shown in Figure 4.

More than 937 images of *Platymonas*, *Chrysophyta*, *Chlorella pyrenoidosa*, *Dunaliella salina*, *Bacillariophyta* and *Symbiodiniaceae* have been captured individually by using a 40× microscope objective (CFI PlanFluor, NA = 0.45).

The software of Labelme, a commonly used graphical image annotation tool, was used to annotate the total dataset manually. The labeling results of different species can be seen in Figure 4. After the annotation for the first time,

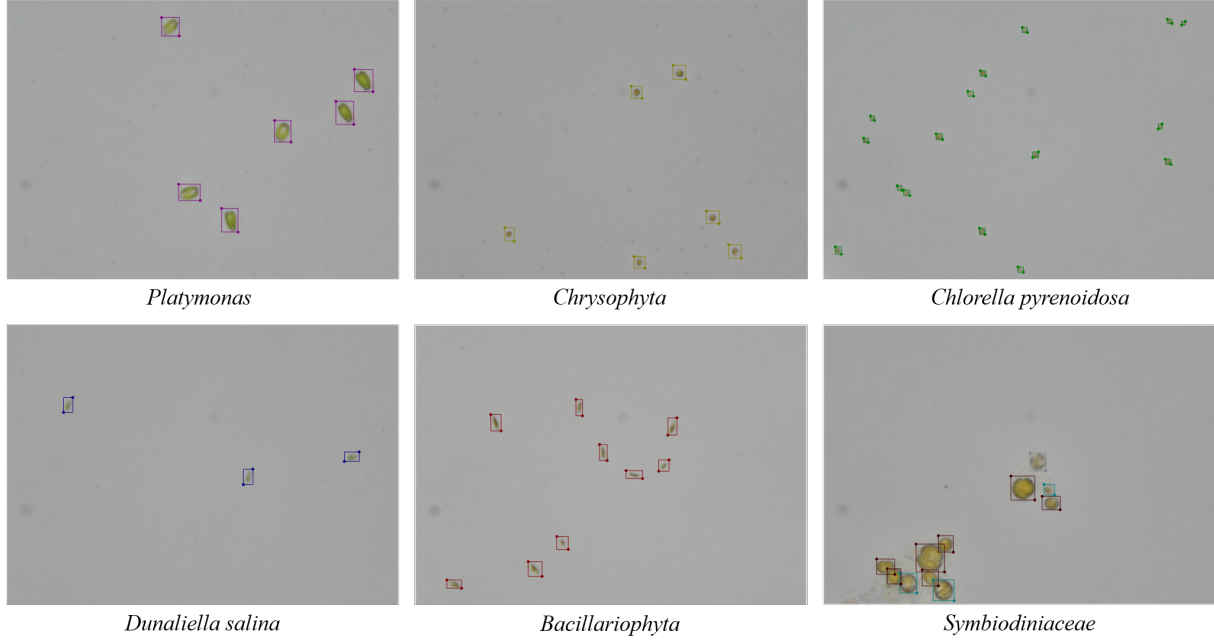


Figure 4: Examples of the labeling results for microalgae objects by using Labelme Software in the training set

another researcher proofread them using Labelme. The original labeling results were saved as files in JSON format and were converted into txt files in YOLO annotation format for the convenience of implementing object detection algorithms. The original images were in TIFF format and were converted into PNG format.

3.3 Dataset Splitting

The total number of images in the dataset is 937 and all the objects in these images were annotated. The total number of annotated objects is 4201. The annotated dataset contains 150 microscopic images of each of the five algae classes *Platymonas*, *Chrysophyta*, *Chlorella pyrenoidosa*, *Dunaliella salina*, and *Symbiodiniaceae*, 40 of class *Bacillariophyta*, and 197 of mixed samples. We split the image set of a single species sample into a training set and a testing set at a scale of 0.7 and all mixed samples are in the testing set. The training set contains 537 images and the testing set contains 430 images, as shown in Figure 5. The total microalgae targets are 2098 in the training set and 2103 in the testing set. The specific number of targets in different categories in the training set and testing set is shown in Figure 6. The resolution of images in the dataset is 2880×2048.

We put all mixed samples in the testing set to increase the difficulties of detection in the potential challenge will be held. And many existing open source algae datasets are of single species, while images from collected water samples in actual practice are mixed species. An algorithm trained on a training set containing a single species of algae and performing well on a test set containing mixed algal images would potentially leverage existing public datasets.

The size of the test set is close to the training set. In actual operation, the process of water collection, image acquisition, and labeling are time-consuming, significantly when the number of algae further increases; it is also expected to get an algorithm that can still perform well when training on a relatively small training set.

This data set can be got accessed via. The license of this dataset is GPL-3.0.

4 Experiments

We trained and tested some classical and the state of the art object detection models on our dataset. We hope these experiments can also offer researchers some hints for continuing research.

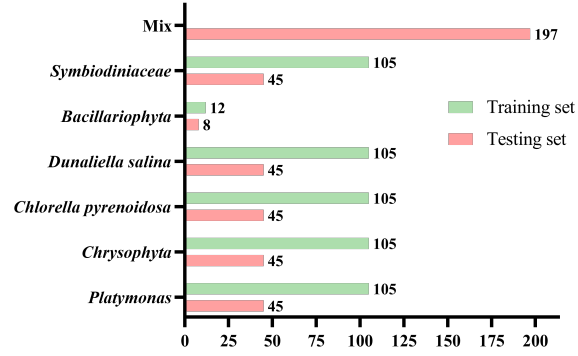


Figure 5: Images counting of different species in the training set and the testing set

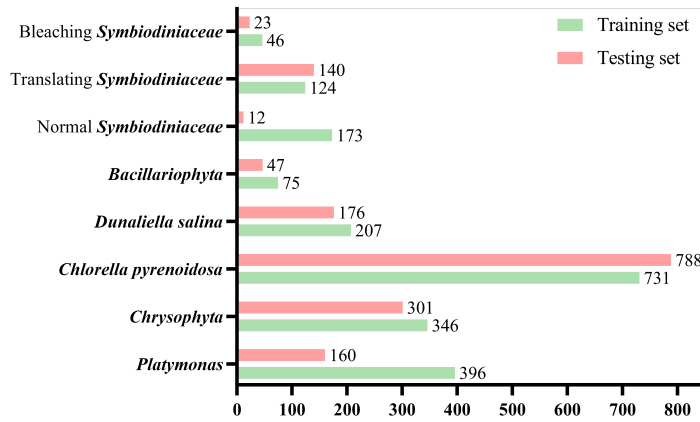


Figure 6: Targets counting in annotated images of different species in the training set and the testing set

4.1 Implementation Details

All experiments were done on RTX A5000 GPU platforms with 24G RAMs. The deep learning framework used is PyTorch [49, 50]. We trained and tested models based on the mmdetection toolbox [51] for the fairness of comparison. The training set in our dataset was split into two sets for training and validation. The new training set contains 429 images, and the validation set contains 108.

We used Min IoU Random Crop, Random Flip, and Photometric Distortion for augmentation in the training process and Multi-Scale Flipping and Random Flipping for augmentation in the testing process.

The sizes of input images in training, validation, and testing are 608×608. The stochastic gradient descent (SGD) optimizer was used in experiments. The learning rate was 0.001, the momentum was 0.9 and the weight decay is 0.0005.

4.2 Evaluation Metrics

Intersection over Union (IoU) is a common metric in object detection, and refers to the intersection ratio between the bounding box predicted by the model and the Ground Truth, which is defined as:

$$IoU(A, B) = \frac{A \cap B}{A \cup B} \quad (1)$$

where A and B represent the area of the bounding box and ground truth predicted by the model, respectively, the detection is considered correct when the IoU is more significant than a certain threshold.

Table 2: Results of different object detection methods on this dataset

Methods	Backbone	mAP(IoU=0.5)	mAP(IoU=0.5:0.95)
Faster-RCNN [29]	ResNet50 [52]	0.584	0.323
Faster-RCNN	ResNet101 [52]	0.630	0.338
Faster-RCNN	Swin-T [53]	0.641	0.328
SSD [34]	VGG16 [54]	0.702	0.360
YOLOv3 [38]	DarkNet-53	0.552	0.257
FCOS [55]	ResNet50	0.246	0.107
TOOD [42]	ResNet50	0.709	0.425

TP means True Positive prediction, TN means True Negative prediction, FP means False Positive prediction, and FN means False Negative prediction. Then, the performance of the model can be evaluated by Precision (P), Recall (R), and average precision (AP), as in:

$$Precision = \frac{TP}{TP + FP} \quad (2)$$

$$Recall = \frac{TP}{TP + FN} \quad (3)$$

Average precision is the area under the precision-recall curve. The mean average precision (mAP) is calculated by finding the Average Precision(AP) for each class and then the average over all classes:

$$mAP = \frac{1}{N} \sum_{i=1}^N AP_i \quad (4)$$

The evaluation metric in validation is mAP(0.50:0.95) to select the best model and we gave the mAP(0.50:0.95) as well as mAP(0.50) results on the testing set. The mAP(0.50:0.95) represents the average mAP over different IoU thresholds (from 0.5 to 0.95 in steps of 0.05) and the mAP(0.50) represents the average mAP over 0.5.

4.3 Results

The detection results on the testing set are shown in Table 2. In our experiments, TOOD [42] algorithm performed best on the testing set after trained 100 epochs. The visualizations of detection results on the testing set are shown in Figure 7. The failure of TOOD method may result from the problems of code base in mmdetection.

5 Conclusions

In this paper, we introduced a new dataset for marine microalgae detection in microscopy images and the building process, including data collection, microscopic imaging, image annotation, proofreading and splitting. This dataset contains microalgae images of 6 species known as *Bacillariophyta*, *Chlorella pyrenoidosa*, *Platymonas*, *Dunaliella salina*, *Chrysophyta*, *Symbiodiniaceae*. Besides, we also collected the images of *Symbiodiniaceae* in different physiological states known as normal, bleaching and translating, which can be an indicator of the situation of coral and its water environment. The dataset contains 967 images, among which 537 are in the training set and 430 in the testing set.

We trained and tested some classical or the state of the art models on our dataset. The main challenges of this task can be concluded as follows:

- High-resolution images and tiny objects
- Small training set size that is close to the testing set
- Multiple species in some images in the testing set
- Class imbalance in the training set

For future research, we will make a larger dataset as the next version and also continue to develop stronger baselines for the microalgae detection tasks. We are also planning a detection algorithm challenge based on this dataset.

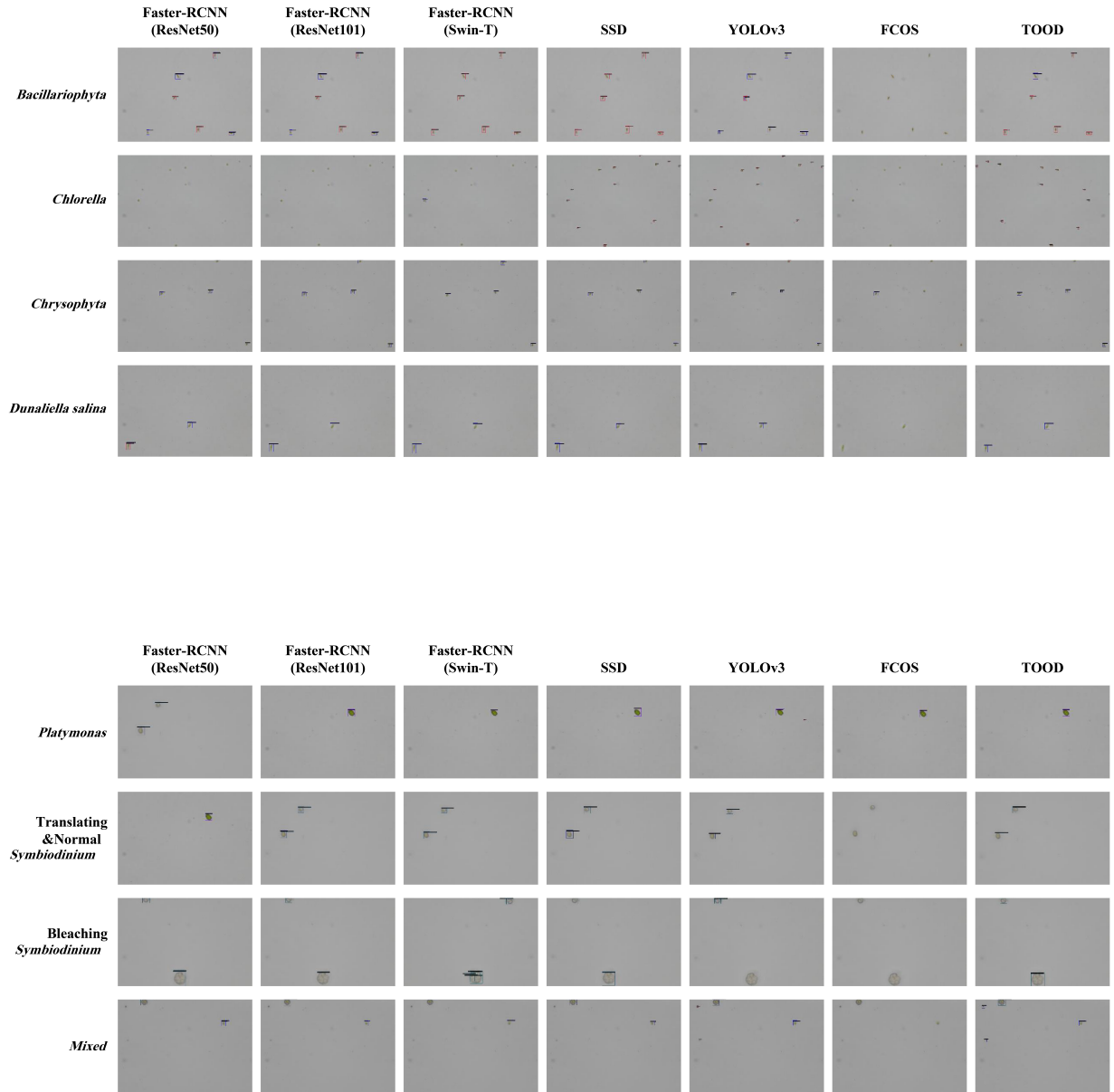


Figure 7: The visualizations of detection results of different methods on the testing set

References

- [1] Xiangning Lu, Yulin Cui, Yuting Chen, Yupeng Xiao, Xiaojin Song, Fengzheng Gao, Yun Xiang, Congcong Hou, Jun Wang, Qinhuo Gan, et al. Sustainable development of microalgal biotechnology in coastal zone for aquaculture and food. *Science of the Total Environment*, 780:146369, 2021.
- [2] Yandu Lu, Qinhuo Gan, Masakazu Iwai, Alessandro Alboresi, Adrien Burlacot, Oliver Dautermann, Hiroko Takahashi, Thien Crisanto, Gilles Peltier, Tomas Morosinotto, et al. Role of an ancient light-harvesting protein of psi in light absorption and photoprotection. *Nature communications*, 12(1):1–10, 2021.
- [3] Franck Gilbert, François Galgani, and Yvon Cadiou. Rapid assessment of metabolic activity in marine microalgae: application in ecotoxicological tests and evaluation of water quality. *Marine Biology*, 112(2):199–205, 1992.
- [4] Alberto Domenighini and Mario Giordano. Fourier transform infrared spectroscopy of microalgae as a novel tool for biodiversity studies, species identification, and the assessment of water quality 1. *Journal of phycology*, 45(2):522–531, 2009.
- [5] Trishala K Parmar, Deepak Rawtani, and YK Agrawal. Bioindicators: the natural indicator of environmental pollution. *Frontiers in life science*, 9(2):110–118, 2016.
- [6] Sarah Naughton, Siobhán Kavanagh, Mark Lynch, and Neil J Rowan. Synchronizing use of sophisticated wet-laboratory and in-field handheld technologies for real-time monitoring of key microalgae, bacteria and physicochemical parameters influencing efficacy of water quality in a freshwater aquaculture recirculation system: A case study from the republic of ireland. *Aquaculture*, 526:735377, 2020.
- [7] Angela Paul Peter, Kuan Shiong Khoo, Kit Wayne Chew, Tau Chuan Ling, Shih-Hsin Ho, Jo-Shu Chang, and Pau Loke Show. Microalgae for biofuels, wastewater treatment and environmental monitoring. *Environmental Chemistry Letters*, 19(4):2891–2904, 2021.
- [8] Jiaoyun Jiang, Aoqi Wang, Xiangzi Deng, Wenxu Zhou, Qinhuo Gan, and Yandu Lu. How symbiodiniaceae meets the challenges of life during coral bleaching. *Coral Reefs*, 40(4):1339–1353, 2021.
- [9] Virginia M Weis. Cellular mechanisms of cnidarian bleaching: stress causes the collapse of symbiosis. *Journal of Experimental Biology*, 211(19):3059–3066, 2008.
- [10] David J Suggett and David J Smith. Coral bleaching patterns are the outcome of complex biological and environmental networking. *Global Change Biology*, 26(1):68–79, 2020.
- [11] Zhenjun Qin, Kefu Yu, Biao Chen, Yinghui Wang, Jiayuan Liang, Wenwen Luo, Lijia Xu, and Xueyong Huang. Diversity of symbiodiniaceae in 15 coral species from the southern south china sea: potential relationship with coral thermal adaptability. *Frontiers in microbiology*, 10:2343, 2019.
- [12] Primo Coltelli, Laura Barsanti, Valtere Evangelista, Anna Maria Frassanito, and Paolo Gualtieri. Water monitoring: automated and real time identification and classification of algae using digital microscopy. *Environmental Science: Processes & Impacts*, 16(11):2656–2665, 2014.
- [13] Sansoen Promdaen, Pakaket Wattuya, and Nuttha Sanevas. Automated microalgae image classification. *Procedia Computer Science*, 29:1981–1992, 2014.
- [14] Jhony-Heriberto Giraldo-Zuluaga, Augusto Salazar, German Diez, Alexander Gomez, Tatiana Martínez, Jesús Francisco Vargas, and Mariana Peñuela. Automatic identification of scenedesmus polymorphic microalgae from microscopic images. *Pattern Analysis and Applications*, 21(2):601–612, 2018.
- [15] Laura Barsanti, Lorenzo Birindelli, and Paolo Gualtieri. Water monitoring by means of digital microscopy identification and classification of microalgae. *Environmental Science: Processes & Impacts*, 2021.
- [16] Ronny Reimann, Bo Zeng, Martin Jakopec, Michał Burdukiewicz, Ingolf Petrick, Peter Schierack, and Stefan Rödiger. Classification of dead and living microalgae *Chlorella vulgaris* by bioimage informatics and machine learning. *Algal research*, 48:101908, 2020.
- [17] Muzhen Xu, Jeffrey Harmon, Dan Yuan, Sheng Yan, Cheng Lei, Kotaro Hiramatsu, Yuqi Zhou, Mun Hong Loo, Tomohisa Hasunuma, Akihiro Isozaki, et al. Morphological indicator for directed evolution of *Euglena gracilis* with a high heavy metal removal efficiency. *Environmental Science & Technology*, 55(12):7880–7889, 2021.
- [18] Jungsu Park, Jiwon Baek, Kwangtae You, Seung Won Nam, and Jongrack Kim. Microalgae detection using a deep learning object detection algorithm, yolov3. *Journal of Korean Society on Water Environment*, 37(4):275–285, 2021.
- [19] Mengying Cao, Junsheng Wang, Yantong Chen, and Yuezhu Wang. Detection of microalgae objects based on the improved yolov3 model. *Environmental Science: Processes & Impacts*, 23(10):1516–1530, 2021.

- [20] Pedro F Felzenszwalb, Ross B Girshick, David McAllester, and Deva Ramanan. Object detection with discriminatively trained part-based models. *IEEE transactions on pattern analysis and machine intelligence*, 32(9):1627–1645, 2010.
- [21] Zhong-Qiu Zhao, Peng Zheng, Shou-tao Xu, and Xindong Wu. Object detection with deep learning: A review. *IEEE transactions on neural networks and learning systems*, 30(11):3212–3232, 2019.
- [22] VIOLA and CVPR2001 JONES. Rapid object detection using a boosted cascade of simple features. *Proceedings of IEEE Conference on Computer Vision and Pattern Recognition, Kauai, Hawaii, U SA*, 2001.
- [23] Paul Viola and Michael J Jones. Robust real-time face detection. *International journal of computer vision*, 57(2):137–154, 2004.
- [24] Navneet Dalal and Bill Triggs. Histograms of oriented gradients for human detection. In *2005 IEEE computer society conference on computer vision and pattern recognition (CVPR'05)*, volume 1, pages 886–893. Ieee, 2005.
- [25] Pedro Felzenszwalb, David McAllester, and Deva Ramanan. A discriminatively trained, multiscale, deformable part model. In *2008 IEEE conference on computer vision and pattern recognition*, pages 1–8. Ieee, 2008.
- [26] Ross Girshick, Jeff Donahue, Trevor Darrell, and Jitendra Malik. Region-based convolutional networks for accurate object detection and segmentation. *IEEE transactions on pattern analysis and machine intelligence*, 38(1):142–158, 2015.
- [27] Kaiming He, Xiangyu Zhang, Shaoqing Ren, and Jian Sun. Spatial pyramid pooling in deep convolutional networks for visual recognition. *IEEE transactions on pattern analysis and machine intelligence*, 37(9):1904–1916, 2015.
- [28] Ross Girshick. Fast r-cnn. In *Proceedings of the IEEE international conference on computer vision*, pages 1440–1448, 2015.
- [29] Shaoqing Ren, Kaiming He, Ross Girshick, and Jian Sun. Faster r-cnn: Towards real-time object detection with region proposal networks. *Advances in neural information processing systems*, 28, 2015.
- [30] Zhaowei Cai and Nuno Vasconcelos. Cascade r-cnn: Delving into high quality object detection. In *Proceedings of the IEEE conference on computer vision and pattern recognition*, pages 6154–6162, 2018.
- [31] Hongkai Zhang, Hong Chang, Bingpeng Ma, Naiyan Wang, and Xilin Chen. Dynamic R-CNN: Towards high quality object detection via dynamic training. *arXiv preprint arXiv:2004.06002*, 2020.
- [32] Peize Sun, Rufeng Zhang, Yi Jiang, Tao Kong, Chenfeng Xu, Wei Zhan, Masayoshi Tomizuka, Lei Li, Zehuan Yuan, Changhu Wang, and Ping Luo. SparseR-CNN: End-to-end object detection with learnable proposals. *arXiv preprint arXiv:2011.12450*, 2020.
- [33] Joseph Redmon, Santosh Divvala, Ross Girshick, and Ali Farhadi. You only look once: Unified, real-time object detection. In *Proceedings of the IEEE conference on computer vision and pattern recognition*, pages 779–788, 2016.
- [34] Wei Liu, Dragomir Anguelov, Dumitru Erhan, Christian Szegedy, Scott Reed, Cheng-Yang Fu, and Alexander C Berg. Ssd: Single shot multibox detector. In *European conference on computer vision*, pages 21–37. Springer, 2016.
- [35] Tsung-Yi Lin, Piotr Dollár, Ross Girshick, Kaiming He, Bharath Hariharan, and Serge Belongie. Feature pyramid networks for object detection. In *Proceedings of the IEEE conference on computer vision and pattern recognition*, pages 2117–2125, 2017.
- [36] Joseph Redmon and Ali Farhadi. Yolo9000: better, faster, stronger. In *Proceedings of the IEEE conference on computer vision and pattern recognition*, pages 7263–7271, 2017.
- [37] Hei Law and Jia Deng. Cornernet: Detecting objects as paired keypoints. In *15th European Conference on Computer Vision, ECCV 2018*, pages 765–781. Springer Verlag, 2018.
- [38] Joseph Redmon and Ali Farhadi. Yolov3: An incremental improvement. *arXiv preprint arXiv:1804.02767*, 2018.
- [39] Alexey Bochkovskiy, Chien-Yao Wang, and Hong-Yuan Mark Liao. Yolov4: Optimal speed and accuracy of object detection. *arXiv preprint arXiv:2004.10934*, 2020.
- [40] Glenn Jocher. yolov5. Github Repository, 2021. <https://github.com/ultralytics/yolov5>.
- [41] Zheng Ge, Songtao Liu, Feng Wang, Zeming Li, and Jian Sun. Yolox: Exceeding yolo series in 2021. *arXiv preprint arXiv:2107.08430*, 2021.
- [42] Chengjian Feng, Yujie Zhong, Yu Gao, Matthew R Scott, and Weilin Huang. Toood: Task-aligned one-stage object detection. In *ICCV*, 2021.

- [43] Nicolas Carion, Francisco Massa, Gabriel Synnaeve, Nicolas Usunier, Alexander Kirillov, and Sergey Zagoruyko. End-to-end object detection with transformers. In *European conference on computer vision*, pages 213–229. Springer, 2020.
- [44] Tsung-Yi Lin, Michael Maire, Serge Belongie, James Hays, Pietro Perona, Deva Ramanan, Piotr Dollár, and C Lawrence Zitnick. Microsoft coco: Common objects in context. In *European conference on computer vision*, pages 740–755. Springer, 2014.
- [45] Mark Everingham, Luc Van Gool, Christopher KI Williams, John Winn, and Andrew Zisserman. The pascal visual object classes (voc) challenge. *International journal of computer vision*, 88(2):303–338, 2010.
- [46] Andrew G Howard, Menglong Zhu, Bo Chen, Dmitry Kalenichenko, Weijun Wang, Tobias Weyand, Marco Andreetto, and Hartwig Adam. Mobilenets: Efficient convolutional neural networks for mobile vision applications. *arXiv preprint arXiv:1704.04861*, 2017.
- [47] MD Guiry. Algaebase. world-wide electronic publication. <http://www.algaebase.org>, 2013.
- [48] Benjamin R Gordon and William Leggat. Symbiodinium—vertebrate symbioses and the role of metabolomics. *Marine drugs*, 8(10):2546–2568, 2010.
- [49] Adam Paszke, Sam Gross, Soumith Chintala, Gregory Chanan, Edward Yang, Zachary DeVito, Zeming Lin, Alban Desmaison, Luca Antiga, and Adam Lerer. Automatic differentiation in pytorch. 2017.
- [50] Adam Paszke, Sam Gross, Francisco Massa, Adam Lerer, James Bradbury, Gregory Chanan, Trevor Killeen, Zeming Lin, Natalia Gimelshein, Luca Antiga, et al. Pytorch: An imperative style, high-performance deep learning library. *Advances in neural information processing systems*, 32, 2019.
- [51] Kai Chen, Jiaqi Wang, Jiangmiao Pang, Yuhang Cao, Yu Xiong, Xiaoxiao Li, Shuyang Sun, Wansen Feng, Ziwei Liu, Jiarui Xu, et al. Mmdetection: Open mmlab detection toolbox and benchmark. *arXiv preprint arXiv:1906.07155*, 2019.
- [52] Kaiming He, Xiangyu Zhang, Shaoqing Ren, and Jian Sun. Deep residual learning for image recognition. In *Proceedings of the IEEE conference on computer vision and pattern recognition*, pages 770–778, 2016.
- [53] Ze Liu, Yutong Lin, Yue Cao, Han Hu, Yixuan Wei, Zheng Zhang, Stephen Lin, and Baining Guo. Swin transformer: Hierarchical vision transformer using shifted windows. In *Proceedings of the IEEE/CVF International Conference on Computer Vision*, pages 10012–10022, 2021.
- [54] Karen Simonyan and Andrew Zisserman. Very deep convolutional networks for large-scale image recognition. *arXiv preprint arXiv:1409.1556*, 2014.
- [55] Zhi Tian, Chunhua Shen, Hao Chen, and Tong He. Fcos: Fully convolutional one-stage object detection. In *Proceedings of the IEEE/CVF international conference on computer vision*, pages 9627–9636, 2019.